

Diffusion of Platinum Ions and Platinum Nanoparticles during Photoreduction Processes Using the Transient Grating Method

Masafumi Harada,^{*,†} Koichi Okamoto,[‡] and Masahide Terazima[§]

Department of Health Science and Clothing Environment, Faculty of Human Life and Environment, Nara Women's University, Nara 630-8506, and Department of Electronic Science and Engineering, Graduate School of Engineering, and Department of Chemistry, Graduate School of Science, Kyoto University, Kyoto 606-8501, Japan

Received June 9, 2006. In Final Form: August 2, 2006

The photoreduction process of PtCl_6^{2-} to Pt nanoparticles in poly(*N*-vinyl-2-pyrrolidone) solutions upon UV light irradiation was investigated by monitoring the change in the diffusion coefficient (D). The D values of chemical species during UV irradiation was measured by the laser-induced transient grating (TG) method. The TG signal of the PtCl_6^{2-} solution before UV irradiation was composed of three kinds of contributions, the thermal grating, the species grating due to the creation of PtCl_4^{2-} , and the species grating due to the depletions of PtCl_6^{2-} . Upon UV irradiation of the solution, the species grating signal due to PtCl_6^{2-} diminished and then the TG signal of Pt nanoparticles gradually appeared. This result indicates that the gradual clustering of Pt^0 atoms into Pt nanoparticles occurs after all PtCl_6^{2-} ions are photochemically reduced to PtCl_4^{2-} and subsequently transformed to Pt^0 atoms with a short delay. With increasing time of the UV irradiation, the TG signal intensity increased, while D of the Pt nanoparticles did not change. This suggests that the number of Pt nanoparticles increases, but the size of the Pt nanoparticles with the polymer layer is unchanged, in the course of the UV irradiation.

1. Introduction

Synthesis of colloidal dispersions of metallic nanoparticles is an interesting field in solid-state chemistry. Because of their small size, these crystallites exhibit novel material properties which largely differ from the bulk properties.^{1–3} The physical and chemical properties of small metal nanoparticles are strongly dependent on the particle size^{4–6} and particle morphology.^{7–9} For preparation of metal nanoparticles, metal ions have often been reduced in protective media to prevent the metal nanoparticles from aggregating. As protective media for colloidal dispersions, water-soluble polymers^{10–12} such as poly(vinyl alcohol), poly(*N*-vinyl-2-pyrrolidone) (PVP), and poly(methyl vinyl ether) have often been used. Pt and Au colloidal dispersions,

which are very active catalysts for hydrogenation or oxidation, have been prepared by the photoreduction of $\text{H}_2\text{PtCl}_6 \cdot 6\text{H}_2\text{O}$ ^{13–15} and $\text{HAuCl}_4 \cdot 4\text{H}_2\text{O}$,¹⁶ respectively, in the presence of stabilizers such as polymers and surfactants. The final size and structure of these metal particles depend on the mechanism of the nucleation and growth process of the metal particles.^{17–19} Although it is evidenced from the UV–vis absorption behavior that the formation of the metal particle proceeds by means of the photoreduction, the rate of photoreduction in the time domain as well as the particle size changes of the metal particles during the reaction has not been clarified yet. Especially, it should be quantitatively elucidated whether the reduction of PtCl_6^{2-} to PtCl_4^{2-} and the particle growth by the association of Pt–Pt bond occur concurrently or whether the particle growth occurs after the reduction of PtCl_6^{2-} to PtCl_4^{2-} is completed. However, it has been difficult to investigate the reduction process of metal ions and the particle formation mechanism in the time domain during the reaction because of the lack of a suitable experimental technique. One of the aims of this study is determination of the reduction and particle formation mechanisms in polymer solutions as well as observation of the change of the average particle size in the polymer solution during the photoreduction by using a diffusion detection method.

The translational diffusion process in solution is one of the most fundamental processes in chemistry and physics. Although there are several methods used for the measurement of the diffusion coefficient (D), measuring D during a fast reaction is still reputed to be difficult. Recently, a transient grating (TG) technique^{20–32} has been recognized gradually as a direct and sensitive method to study diffusion processes.

* To whom correspondence should be addressed. Phone and fax: +81-742-20-3466. E-mail: harada@cc.nara-wu.ac.jp.

† Nara Women's University.

‡ Graduate School of Engineering, Kyoto University. Present address: California Institute of Technology, Mail Code 136-93, Pasadena, CA 91125.

§ Graduate School of Science, Kyoto University.

(1) Feldheim, D. L.; Foss, C. A., Jr. *Metal Nanoparticles: Synthesis, Characterization, and Applications*; Marcel Dekker: New York, 2002.

(2) Kreibitz, U.; Vollmer, M. *Optical Properties of Small Metal Clusters*; Springer-Verlag: Berlin, 1995.

(3) Pelizzetti, E. *Fine Particles Science and Technology—From Micro to New Particles*; Kluwer Academic Publishers: Dordrecht, The Netherlands, 1996.

(4) Teranishi, T.; Hosoe, M.; Tanaka, T.; Miyake, M. *J. Phys. Chem. B* **1999**, *103*, 3818.

(5) Leff, D. V.; Ohara, P. C.; Heath, J. R.; Gelbart, W. M. *J. Phys. Chem.* **1995**, *99*, 7036.

(6) Motte, L.; Billoudet, F.; Lacaze, E.; Douin, J.; Pileni, M. P. *J. Phys. Chem. B* **1997**, *101*, 138.

(7) Ahmadi, T. S.; Wang, Z. L.; Green, T. C.; Henglein, A.; El-Sayed, M. A. *Science* **1996**, *272*, 1924.

(8) Ahmadi, T. S.; Wang, Z. L.; Henglein, A.; El-Sayed, M. A. *Chem. Mater.* **1996**, *8*, 1161.

(9) Petroski, J. M.; Wang, Z. L.; Green, T. C.; El-Sayed, M. A. *J. Phys. Chem. B* **1998**, *102*, 3316.

(10) Duff, D. G.; Edwards, P. P.; Johnson, B. F. G. *J. Phys. Chem.* **1995**, *99*, 15934.

(11) Huang, H. H.; Ni, X. P.; Loy, G. L.; Chew, C. H.; Tan, K. L.; Loh, F. C.; Deng, J. F.; Xu, G. Q. *Langmuir* **1996**, *12*, 909.

(12) Itakura, T.; Torigoe, K.; Esumi, K. *Langmuir* **1995**, *11*, 4129.

(13) Toshima, N.; Takahashi, T. *Bull. Chem. Soc. Jpn.* **1992**, *65*, 400.

(14) Toshima, N.; Nakata, K.; Kitoh, H. *Inorg. Chim. Acta* **1997**, *265*, 149.

(15) Einaga, H.; Harada, M. *Langmuir* **2005**, *21*, 2578.

(16) Qiu, J.; Jiang, X.; Zhu, C.; Shirai, M.; Si, J.; Jiang, N.; Hirao, K. *Angew. Chem., Int. Ed.* **2004**, *43*, 2230.

(17) Park, J.; Privman, V.; Matijevec, E. *J. Phys. Chem. B* **2001**, *105*, 11630.

(18) Ershov, B. G.; Henglein, A. *J. Phys. Chem. B* **1998**, *102*, 10663.

(19) Ershov, B. G.; Henglein, A. *J. Phys. Chem. B* **1998**, *102*, 10667.

In the TG experiment,²³ a sinusoidal pattern is created by the interference of two excitation beams. If a sample contains photochemically active molecules and they are converted to other species in the bright region, this space-selective excitation induces a spatially modulated distribution of chemical species that causes a spatially modulated refractive index and/or absorbance. This modulation (grating) diffracts another probe beam entering this region. The signal decays as the modulation smears out by the diffusion. Therefore, the decay of the TG signal reflects the diffusion process of the probe molecule. Since this method has a very fast time response, the TG method has been applied to measurements of D of short-lived radicals,^{24–26} intermediates of protein reactions,^{27–31} or molecules in polymer solutions.

In this paper, we demonstrate that the TG technique is a convenient and useful method to determine D of Pt ionic species and Pt nanoparticles in polymer solutions during the Pt particle formation process. We measured the TG signal of Pt ionic species and Pt nanoparticles in PVP polymer solutions under UV light irradiation for various durations. The temporal profile of the signal changed drastically upon UV irradiation. We determined D of the intermediate chemical species in the early stage of the photoreduction to create Pt nanoparticles with polymer layers. On the basis of these results, we discussed the Pt particle formation mechanism.

2. Principles

The TG signal is created in a sample solution by crossing two coherent excitation beams with an angle θ . The light intensity in the crossing region is modulated by the interference as

$$I(x,t) = I(t)[1 + \cos(2\pi x/\Lambda)]/2 \quad (1)$$

where $I(x,t)$ is the power of the excitation laser, the fringe spacing Λ is given by

$$\Lambda = \lambda_{\text{ex}}/[2 \sin(\theta/2)] \quad (2)$$

and λ_{ex} is the wavelength of the excitation light. Since we are interested in the TG signal on a time scale much longer than the pulse width of the excitation beam, $I(t)$ is considered to be the δ function of t :

$$I(t) = I_0\delta(t) \quad (3)$$

By the spatially modulated light due to the interference between two light beams, chemical species in a sample are excited to excited states in which photochemical reductions take place in proportion to the light intensity $I(x,t)$. Since the created species usually have different optical properties (such as absorption coefficients and refractive indices), the spatially modulated photoexcitation induces a spatially modulated absorbance (amplitude grating) or refractive index (phase grating) at the probe beam wavelength. The refractive index (n) and absorbance

(k) in the sample solution after the excitation are represented by

$$n(x,t) = n_0 + \delta n_s(x,t) + \delta n_{\text{th}}(x,t) \quad (4)$$

$$k(x,t) = k_0 + \delta k(x,t) \quad (5)$$

where n_0 and k_0 are, respectively, the unperturbed refractive index and absorbance of the solution. The contribution of $\delta n_{\text{th}}(x,t)$ represents the refractive index change (δn) by the thermal expansion of the solution due to the unavoidable radiationless transition from the excited state (thermal grating), and $\delta n_s(x,t)$ represents δn by the spatially modulated distribution of chemical species (species grating). The δk term in eq 5 represents the absorption change due to the chemical species. By solving the diffusion rate equations, we can obtain the following equations, which display the time dependence of the spatial modulations:^{20,21,24}

$$\delta n_{\text{th}}(q,t) = \delta n_{\text{th}}^0 \exp(-D_{\text{th}}q^2t) \quad (6)$$

$$\delta n_s(q,t) = \delta n_s^0 \exp(-Dq^2t) \quad (7)$$

$$\delta k(q,t) = \delta k^0 \exp(-Dq^2t) \quad (8)$$

where q is the grating wavenumber, D_{th} is the thermal diffusivity, D is the diffusion coefficient of the chemical species, and $\delta n_{\text{th}}(q,t)$ and $\delta n_s(q,t)$ are the spatial Fourier components of $\delta n_{\text{th}}(x,t)$ and $\delta n_s(x,t)$, respectively. Since the refractive index decreases with increasing temperature, δn_{th}^0 should be negative. Under the thick grating and the weak diffraction conditions, the TG signal intensity $I_{\text{TG}}(t)$ at grating wavenumber q is represented by

$$I_{\text{TG}}(t) = A(\delta n_{\text{th}}(q,t) + \delta n_s(q,t))^2 + B(\delta k(q,t))^2 \quad (9)$$

where A and B are constants.

3. Experimental Section

3.1. Materials. Colloidal dispersions of Pt particles were synthesized by the photoreduction of PtCl_6^{2-} with the protective polymer PVP. The average molecular weight of PVP used here was 40000. Hexachloroplatinic(IV) acid (hydrated hydrogen hexachloroplatinate(IV), $\text{H}_2\text{PtCl}_6 \cdot 6\text{H}_2\text{O}$; guaranteed reagent, Nacalai Tesque), PVP (K-30, Wako Chemicals), ethanol (guaranteed reagent, 99.5%, Nacalai Tesque), and distilled water were used without further purification.

3.2. TG Measurements. The setup of the TG method has been reported in detail elsewhere.^{20–22,24–30} Briefly, as shown in Figure 1, an excitation beam from an excimer laser [XeCl (308 nm), Lumonics Hyper-400] was split into two beams by a beam splitter. The repetition rate of the excitation pulse was 1–3 Hz, and the pulse width was about 20 ns. These beams were crossed inside a quartz sample cell (10 mm optical path length), and the interference pattern between these beams (optical grating) was created. The laser fluence at the crossing point was measured by a pyroelectric joulemeter (Moletron J3-09), and it was typically ~ 0.3 mJ/cm². The thermal energy released by the nonradiative relaxation raises the temperature of the sample, and it creates the thermal grating. The excited ions partly reacted, and the concentrations of the reactant and products were modulated (species grating). A He–Ne laser was used as a probe beam and brought into the crossing region at the Bragg angle. A diffracted probe beam (the TG signal) was isolated from the excitation beams with a pinhole and a red filter (Toshiba R-60) with a cutoff wavelength of 600 nm. The intensity of the TG signal is detected by a photomultiplier tube (Hamamatsu R-928) and recorded with a digital oscilloscope (Tektronix 2430A). The fringe spacing Λ was calculated from the decay rate of the thermal grating signal of a benzene solution.³² The sample solution was irradiated by a 500 W super-high-pressure mercury lamp to reduce Pt^{4+} ions. The light

(20) Terazima, M.; Okamoto, K.; Hirota, N. *Laser Chem.* **1994**, *13*, 169.

(21) Terazima, M.; Okamoto, K.; Hirota, N. *J. Phys. Chem.* **1993**, *97*, 13387.

(22) Okamoto, K.; Hirota, N.; Terazima, M. *J. Phys. Chem. A* **1997**, *101*, 5380.

(23) Eichler, H. J.; Günter, P.; Pohl, D. W. *Laser induced dynamic gratings*; Springer-Verlag: Berlin, 1986.

(24) Terazima, M.; Hirota, N. *J. Chem. Phys.* **1993**, *98*, 6257.

(25) Okamoto, K.; Terazima, M.; Hirota, N. *J. Chem. Phys.* **1995**, *103*, 10445.

(26) Okamoto, K.; Hirota, N.; Terazima, M. *J. Phys. Chem. A* **1998**, *102*, 3447.

(27) Nada, T.; Terazima, M. *Biophys. J.* **2003**, *85*, 1876.

(28) Nishida, S.; Nada, T.; Terazima, M. *Biophys. J.* **2004**, *87*, 2663.

(29) Nishida, S.; Nada, T.; Terazima, M. *Biophys. J.* **2005**, *89*, 2004.

(30) Eitoku, T.; Nakasone, Y.; Matsuoka, D.; Tokutomi, S.; Terazima, M. *J. Am. Chem. Soc.* **2005**, *127*, 13238.

(31) Terazima, M. *Acc. Chem. Res.* **2000**, *33*, 687.

(32) Terazima, M.; Okamoto, K.; Hirota, N. *J. Phys. Chem.* **1993**, *97*, 5188.

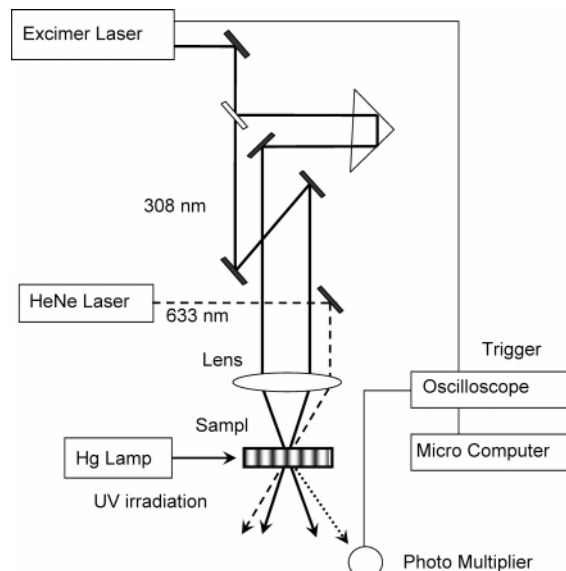


Figure 1. Experimental setup for the TG measurement and the configuration of the excitation and probe beams.

intensity of the mercury lamp is approximately 65 mW/cm^2 . The direction of UV irradiation was perpendicular to that for the TG measurement. The photoreduction of Pt^{4+} ions to create Pt atoms via Pt^{2+} ions occurred mainly due to the UV irradiation process, as reported previously.^{13,15,33} The UV–vis absorption spectra of the prerduced (before irradiation) and the reduced (after irradiation for about 2 h) samples were measured with a Shimadzu UV-2500PC by using quartz cells (1 mm optical path length) to adjust the metal concentration for the UV measurements.

Colloidal dispersions of Pt particles (0.66 mM) were prepared from $\text{H}_2\text{PtCl}_6 \cdot 6\text{H}_2\text{O}$ by irradiation with a 500 W super-high-pressure mercury lamp in a solution of water and ethanol (the volume ratio of water and ethanol is 1/1) containing PVP. The concentration of polymer in water/ethanol (1/1) solutions was varied at $[\text{PVP monomeric unit}]/[\text{metal}] = 4$ and 400, which we call dilute and concentrated polymer solutions, respectively. Briefly, for the preparation of the dilute polymer solution, 5 mL of a 1.32 mM aqueous solution of $\text{H}_2\text{PtCl}_6 \cdot 6\text{H}_2\text{O}$ was added to 5 mL of a 5.28 mM ethanol solution of PVP. N_2 gas was bubbled into the solution, and vigorous stirring was carried out for 10 min to remove the dissolved O_2 . For the preparation of the concentrated polymer solution, 5 mL of a 1.32 mM aqueous solution of $\text{H}_2\text{PtCl}_6 \cdot 6\text{H}_2\text{O}$ was added to 5 mL of a 528 mM ethanol solution of PVP, followed by N_2 bubbling and vigorous stirring.

3.3. Characterization of Pt Particles. Transmission electron microscopy (TEM) images of the colloidal dispersions of Pt nanoparticles were obtained using a JEM-2000FX instrument operated at 200 kV as the acceleration voltage. A high-resolution carbon-supported copper mesh was used to support the samples of colloidal dispersions. The diameter of each particle was determined from enlarged photographs. The particle size distribution and the average diameter were obtained by measuring about 200 particles in arbitrarily chosen areas in the enlarged photograph.

4. Results and Discussion

4.1. Photochemical Formation of Pt Particles from PtCl_6^{2-} in a Dilute PVP Solution. Photoirradiation with UV light of PtCl_6^{2-} complexes in an ethanol/water solution leads to the reduction of Pt^{4+} to Pt^0 metal particles via Pt^{2+} ^{34–36} as described

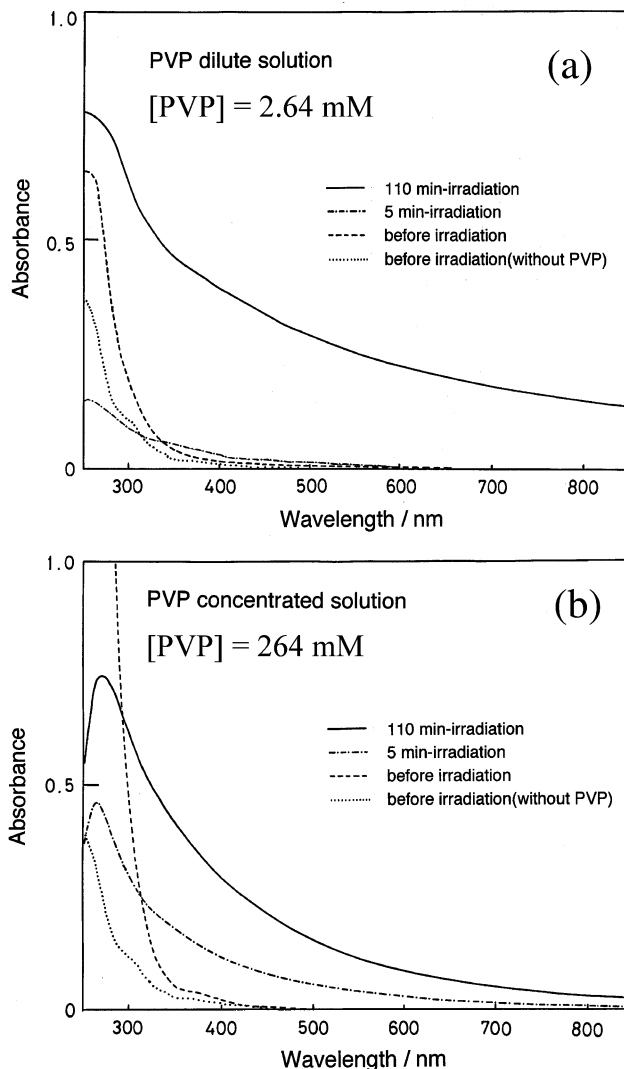
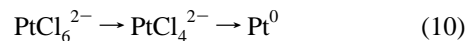


Figure 2. UV–vis absorption spectra of the Pt-containing solutions (ethanol/water, 1/1 (v/v)) before and after UV irradiation (a) in the dilute PVP solution and (b) in the concentrated PVP solution. The photoreduction was carried out for up to 110 min. The spectrum of Pt-containing solutions without PVP is also indicated.

by eq 10. According to NMR studies by Cameron and Bocarsly,



the Pt^0 metal formation does not occur until a $\sim 90\%$ yield of PtCl_4^{2-} has accumulated.³⁶ This finding shows that the increase of the PtCl_6^{2-} concentration decreased the rate for the Pt^0 metal particle formation. This process can be visually monitored by the color change of the solution: the precursor complex PtCl_6^{2-} is yellow, whereas PtCl_4^{2-} is orange. In our experimental condition where a 500 W mercury lamp was used as the light source and UV light in the range of 200–400 nm was used for irradiation of the precursor solution, PtCl_6^{2-} was photochemically reduced to PtCl_4^{2-} within a few minutes and subsequently transformed to metallic species within 60 min, which gave a black colloidal solution.

UV–vis measurements confirmed the reduction of PtCl_6^{2-} by UV irradiation. Parts a and b of Figure 2 show the UV–vis spectra of the Pt solutions with and without the polymer before and after UV irradiation in the case of the dilute and concentrated PVP solutions, respectively. In both cases, photoirradiation was performed for 110 min to complete the Pt reduction. The solution

(33) Harada, M.; Einaga, H. *Langmuir* **2006**, *22*, 2371.

(34) Bocarsly, A. B.; Cameron, R. E.; Zhou, M. In *Proceedings of the Seventh International Symposium on the Photochemistry and Photophysics of Coordination Compounds*; Yersin, H., Volger, A., Eds.; Springer: Berlin, 1987; pp 177–180.

(35) Cameron, R. E.; Bocarsly, A. B. *J. Am. Chem. Soc.* **1985**, *107*, 6116.

(36) Cameron, R. E.; Bocarsly, A. B. *Inorg. Chem.* **1986**, *25*, 2910.

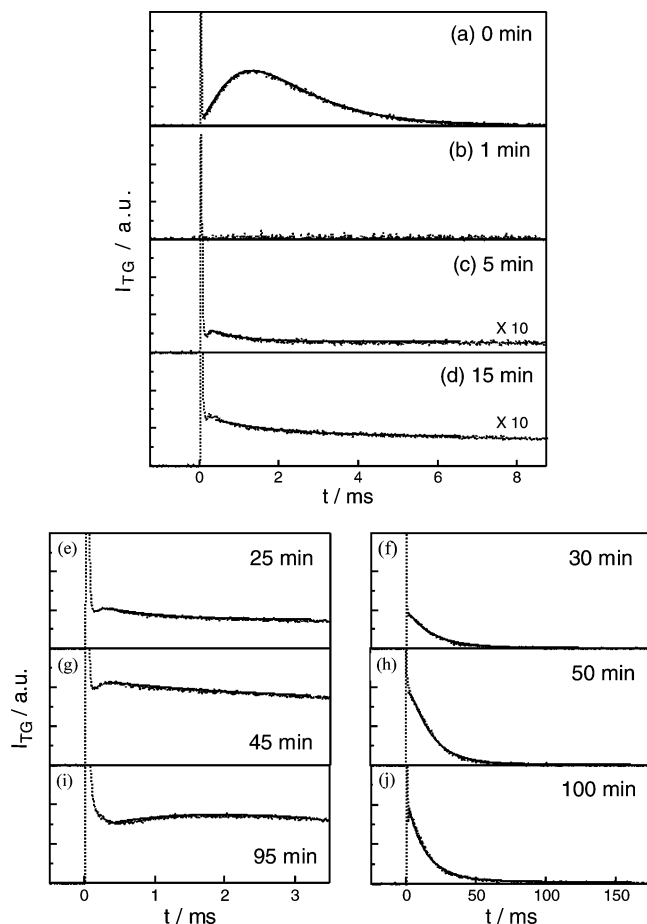


Figure 3. Time dependence of the TG signals (I_{TG}) in water/ethanol (1/1) solutions observed (a) before and (b–j) after UV irradiation. The initial sharp spikelike signal is due to the contribution of the thermal grating. In all the cases, the best fitted curves are drawn as a solid line using (a) eq 12 and (c–j) eq 14 after the complete decay of the thermal grating signal (dashed line). The concentration of polymer was [PVP monomeric unit]/[metal] = 4 (the dilute PVP solution).

containing $PtCl_6^{2-}$ complexes exhibits an LMCT band with a maximum at 262 nm and two bands at around 360 and 480 nm corresponding to d–d transitions, which are slightly solvent dependent.³⁷ Photoirradiation for 110 min resulted in the complete disappearance of the absorption band and a significant increase of the baseline in absorbance. The resulting solution was stable and well dispersed for at least several months. PVP was necessary for the stabilization of Pt nanoparticles and prevented the formation of large aggregates of Pt nanoparticles as a precipitate, not working as a reducing agent in this reaction. Comparing the spectral behavior of dilute PVP solutions (Figure 2a) with that of concentrated PVP solutions (Figure 2b), a similar tendency, that is, the photoreduced samples have a large absorbance at a wavelength longer than 300 nm, was observed despite the difference in intensity due to the particle size.

Figure 3 shows the time dependence of typical temporal profiles of the TG signals before and after UV irradiation for the dilute PVP solutions with Pt ions. The signal obtained from the sample before UV irradiation consists of three components, a spikelike signal, a subsequent slow rise component, and a slow decay, as shown in Figure 3a. The spikelike signal, which decays in a few microseconds, originates from the thermal grating. After the thermal grating signal decays to the baseline completely, the

slower decay of the TG signal with a lifetime of millisecond order appears. The slower rise and decay components should be the species grating created by the photochemical reduction. In this early stage of the photochemical reduction process, two chemical species (Pt^{4+} and Pt^{2+}) could contribute to the TG signal.

The observed TG signal changed drastically upon UV irradiation of the sample. As shown in Figure 3b, the above slower rise and decay components disappeared after irradiation with UV light for 1 min, while the thermal grating signal still remained. After irradiation with UV light for 5 min, as shown in Figure 3c, the TG signal appeared, which has two components; one is the slow decay of millisecond order, and the other is a much slower decay. The signal intensities of this slower decay component become larger with increasing UV irradiation time (Figure 3d). The slower component should be due to the Pt particles, while the millisecond decay component should be due to the Pt ionic species. We found that all of the Pt ionic signal component disappeared before the Pt particle signal began to appear. This behavior suggests that the gradual clustering process of Pt particles occurred once all Pt^{4+} ions were completely reduced to Pt^{2+} . Especially, the decay rate of the Pt ionic species is quite different from that of Pt particles, comparing parts e and f of Figure 3. The species grating relaxes with a shorter time of less than ca. 10 ms and then to the baseline level by diffusion on a long time scale (i.e., about 150 ms) as shown in Figure 3f. This trend of the species grating is observed at a longer reduction time, as shown in Figure 3i,j. After the longer UV irradiation, the components due to the Pt ionic species become smaller and almost disappear at 45 min of irradiation (Figure 3g). On the other hand, the slower signal due to the Pt particles becomes larger, and the decay time becomes slower. This behavior shows that the Pt particles grew larger and larger after the UV irradiation.

The observed TG signals before UV irradiation (Figure 3a) can be decomposed into a thermal grating and chemical species gratings (Pt^{4+} and Pt^{2+}). The absorptions by Pt^{4+} and Pt^{2+} ions at the probe beam wavelength (633 nm) are nearly zero as shown by the UV–vis spectra in Figure 2. Therefore, the TG signal ($I_{TG}(t)$) before UV irradiation is predicted to be expressed by

$$I_{TG}(t) = A[\delta n_{th}^0 \exp(-D_{th}q^2t) + \delta n_{Pt^{2+}}^0 \exp(-D_{Pt^{2+}}q^2t) - \delta n_{Pt^{4+}}^0 \exp(-D_{Pt^{4+}}q^2t)]^2 \quad (11)$$

where $D_{Pt^{2+}}$ and $D_{Pt^{4+}}$ are the diffusion coefficients of Pt^{2+} and Pt^{4+} , respectively. For the refractive index change by the thermal expansion, δn_{th}^0 is negative, which comes from the decrease of density due to the increase of the temperature. By Kramers–Kronig relation and the absorption bands in Figure 2, we can figure out that both $\delta n_{Pt^{2+}}^0$ and $\delta n_{Pt^{4+}}^0$ are positive. As for the spatially modulated distribution of chemical species, the third term in eq 11 has a negative sign because Pt^{4+} is the consumed species, while the second term has a positive sign because Pt^{2+} is produced. From these facts, we found that the fast spikelike component in Figure 3a is negative and the slow rise and decay components are positive and negative, respectively. Therefore, the origins of the spikelike, rise, and decay components are the thermal grating, Pt^{4+} ion, and Pt^{2+} ion, respectively.

In the curve-fitting procedure, the contribution of the thermal grating signals was neglected, because the decay of the thermal grating was much faster than that of the other species grating. Therefore, the time profile of the TG signal in Figure 3a was fitted by

$$I_{TG}(t) = [a_{Pt^{2+}} \exp(-k_{Pt^{2+}}t) - a_{Pt^{4+}} \exp(-k_{Pt^{4+}}t)]^2 \quad (12)$$

(37) Swihart, D. L.; Mason, W. R. *Inorg. Chem.* **1970**, *9*, 1749.

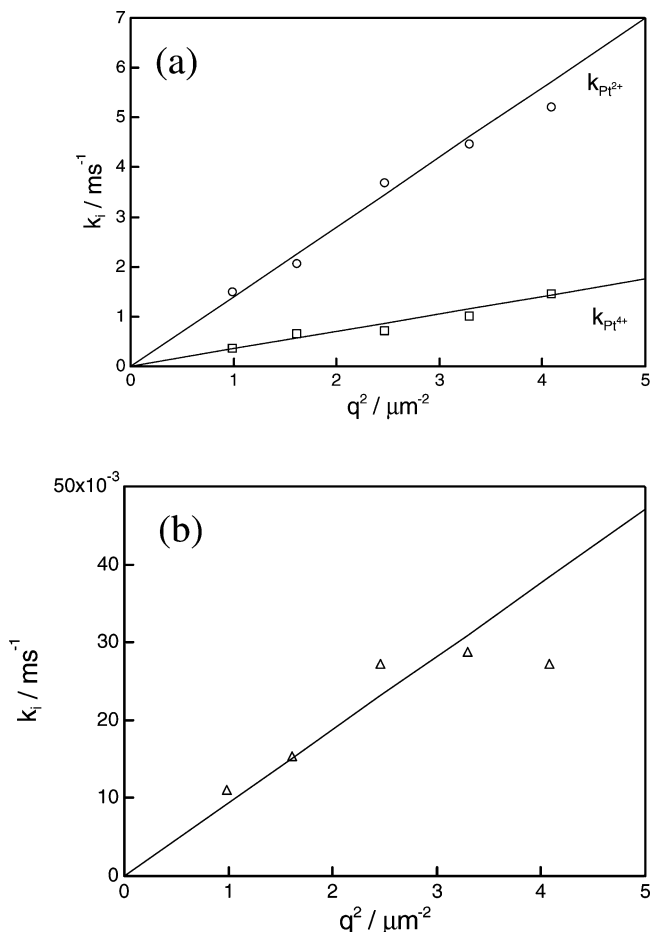


Figure 4. Decay rate constants (k_i) vs q^2 of (a) chemical species (\square) Pt^{4+} and (\circ) Pt^{2+} existing before UV irradiation and (b) Pt particles (\triangle) after 90 min of UV irradiation in the 1/1 solution of water and ethanol containing PVP. The concentration of polymer was [PVP monomeric unit]/[metal] = 4 (the dilute PVP solution).

where $a_{\text{Pt}^{2+}}$ and $a_{\text{Pt}^{4+}}$ are the preexponential factors. By means of the least-squares fitting, the best fitted curve is obtained on the basis of eq 12, which is drawn as a solid line in Figure 3a. The decay rate constants of these signal components ($k_{\text{Pt}^{2+}}$, $k_{\text{Pt}^{4+}}$) in Figure 3a were plotted against q^2 in Figure 4a. Both rate constants depend on the fringe spacing and show a good linear relationship with a negligibly small intercept with the ordinate axis. This linear relationship indicates that eq 11 is indeed a reasonable equation and our analysis method is appropriate. The slope of each line shows the D_i value because the relationship of $k_i = D_i q^2$ is given by eqs 11 and 12. Therefore, $D_{\text{Pt}^{2+}}$ and $D_{\text{Pt}^{4+}}$ were obtained from the slope of Figure 4a.

When the sample is irradiated for 15 min (Figure 3d), the absorption due to the created Pt particle ($\delta k_{\text{particle}}$) becomes a lot stronger than $\delta n_{\text{Pt}^{2+}}$ or $\delta n_{\text{Pt}^{4+}}$. Therefore, this amplitude grating term should be taken into account in the TG signal for the colloidal solution of Pt particles after the UV irradiation, and the temporal profile is predicted to be expressed by

$$I_{\text{TG}}(t) = A[\delta n_{\text{th}}^0 \exp(-D_{\text{th}} q^2 t) + \delta n_{\text{Pt}^{2+}}^0 \exp(-D_{\text{Pt}^{2+}} q^2 t) - \delta n_{\text{Pt}^{4+}}^0 \exp(-D_{\text{Pt}^{4+}} q^2 t)]^2 + B[\delta k_{\text{particle}}^0 \exp(-D_{\text{particle}} q^2 t)]^2 \quad (13)$$

where D_{particle} is the diffusion coefficient of the created Pt particle. δn_{th}^0 is negative as is the case before the UV irradiation, and $\delta k_{\text{particle}}^0$ is positive (Figure 2). Moreover, it is well-known that, in the photoreduction process of PtCl_6^{2-} to PtCl_4^{2-} , the number

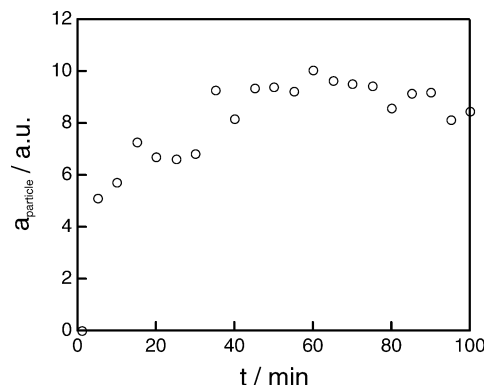


Figure 5. Species grating intensity of the Pt particles (a_{particle}) vs reduction time. The concentration of polymer was [PVP monomeric unit]/[metal] = 4 (the dilute PVP solution).

of Pt^{4+} ions decreases and the number of Pt^{2+} ions increases while the reduction proceeds. Thus, the contribution of Pt^{4+} ions is not pronounced because the Pt^{4+} species is consumed in photoreduction in the course of UV irradiation. Therefore, the decay components on a millisecond scale in Figure 3c–e, g, i are attributed to the Pt^{2+} ionic species, while the slower decay components in Figure 3f, h, j are attributed to the Pt particles.

In the curve-fitting for the TG signal after UV irradiation, the contributions of the thermal grating signals and Pt^{4+} ionic species grating were neglected. Therefore, the TG signals in Figure 3c–j were fitted by

$$I_{\text{TG}}(t) = [a_{\text{Pt}^{2+}} \exp(-k_{\text{Pt}^{2+}} t)]^2 + [a_{\text{particle}} \exp(-k_{\text{particle}} t)]^2 \quad (14)$$

where a_{particle} is the preexponential factor. The best fitted curves by eq 14 are shown in Figure 3c–j. The k_{particle} values are plotted against q^2 in Figure 4b. This plot also shows a good linear relationship with a small intercept. This suggests that the slower decay components are also governed by a diffusion process, and the slope of this plot shows D_{particle} .

Figure 5 shows the plot of the TG signal intensities due to the Pt particles (a_{particle}) obtained by the fitting with eq 14 for the dilute PVP solution vs reduction time during the UV irradiation process. a_{particle} is proportional to $\delta k_{\text{particle}}$. The signal intensity gradually increases with an increase of the reduction time and then becomes almost constant after 60 min. This behavior is consistent with the increase of the UV–vis absorption in the wavelength range between 300 and 850 nm, as shown in Figure 2.

Figure 6 shows the time dependence of D plotted against the reduction time for the dilute PVP solutions containing Pt ions. As previously mentioned, three chemical species are observed during the UV irradiation. The D values of Pt^{2+} (circles) are almost constant ($D_{\text{Pt}^{2+}} = 1.5 \times 10^{-9} \text{ m}^2 \text{ s}^{-1}$) with increasing reduction time, while the signal due to Pt^{4+} (squares) cannot be detected after at least 5 min of reduction. Also, the D values of the Pt particles (triangle) become gradually close to a constant value ($D_{\text{particle}} = 6.0 \times 10^{-11} \text{ m}^2 \text{ s}^{-1}$). This means that the size of the Pt particle produced in the photoreduction does not grow larger in the UV irradiation, and the number of Pt particles increases in this reduction process. The detailed discussion of D values will be shown later.

4.2. Dependence on the PVP Concentration of Photochemical Formation of Pt Particles from PtCl_6^{2-} . To investigate the effect of the protective polymer PVP, we examined photoreduction in two solutions with different polymer concentrations; one is the concentrated PVP solution, and the other is the solution without PVP. Figures 7 and 8 show the time

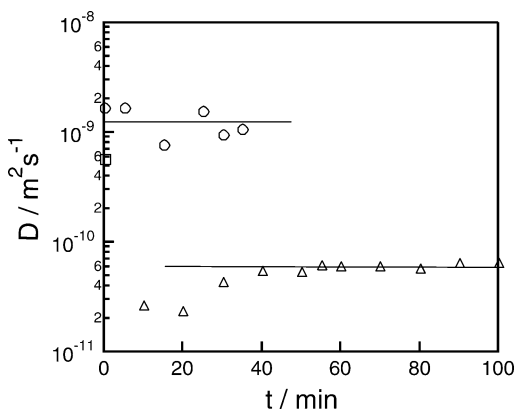


Figure 6. Time evolution of D of the three components produced during UV irradiation: (\square) Pt^{4+} ionic species, (\circ) Pt^{2+} ionic species, and (\triangle) Pt particles. The Pt particles were prepared by UV irradiation in water/ethanol (1/1) solutions of PVP. The concentration of polymer was [PVP monomeric unit]/[metal] = 4 (the dilute PVP solution).

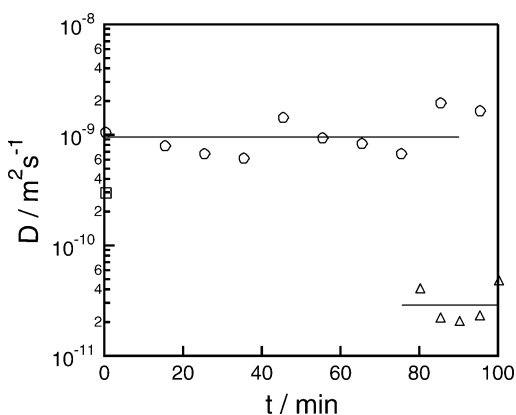


Figure 7. Time evolution of D of the three components produced during UV irradiation: (\square) Pt^{4+} ionic species, (\circ) Pt^{2+} ionic species, and (\triangle) Pt particles. The Pt particles were prepared by UV irradiation in water/ethanol (1/1) solutions of PVP. The concentration of polymer was [PVP monomeric unit]/[metal] = 400 (the concentrated PVP solution).

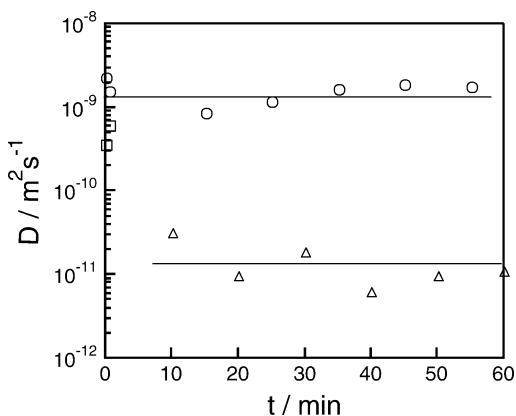


Figure 8. Time evolution of D of the three components produced during UV irradiation: (\square) Pt^{4+} ionic species, (\circ) Pt^{2+} ionic species, and (\triangle) Pt particles. The Pt particles were prepared by UV irradiation in water/ethanol (1/1) solutions without PVP.

dependence of D plotted against the reduction time for the concentrated PVP solutions and the Pt solutions without PVP, respectively, to compare with that of the dilute PVP solutions (Figure 6). The qualitative behaviors are quite similar in these three cases. The time evolutions of the TG signals (not shown in this paper) are also very similar to each other.

Comparing the behavior of Figure 6 with those of Figures 7 and 8, one may note that the species grating signals of Pt^{4+} (squares) disappear in a few minutes (less than 5 min) and the species grating signals of Pt particles (triangles) appear after a longer UV irradiation. In the case of the concentrated PVP solutions shown in Figure 7, the D values of Pt^{2+} (circles) and Pt particles (triangles) are almost constant ($D_{\text{Pt}^{2+}} = 1.0 \times 10^{-9} \text{ m}^2 \text{ s}^{-1}$ and $D_{\text{particle}} = 3.0 \times 10^{-11} \text{ m}^2 \text{ s}^{-1}$, respectively) regardless of the reduction time. It is noteworthy that the TG signal due to the Pt particles appears after UV irradiation for 80 min in the concentrated PVP solutions (Figure 7) while the TG signal due to the Pt particles appears only after irradiation for 10 min in the dilute PVP solutions (Figure 6). This means that the clustering of Pt atoms to create Pt particles is relatively slower in the concentrated solutions than in the dilute solutions. On the other hand, for the Pt ionic solutions without PVP (Figure 8), the D values of Pt^{2+} (circles) are equal to $1.5 \times 10^{-9} \text{ m}^2 \text{ s}^{-1}$ and the D values of Pt particles (triangles) become gradually close to the value $D_{\text{particle}} = 1.0 \times 10^{-11} \text{ m}^2 \text{ s}^{-1}$. Hence, we can say that the D values of the Pt particles created in the concentrated PVP solutions are similar to those created in the dilute PVP solutions, but they are much larger than those created in solutions without PVP. On the other hand, the D values of Pt^{2+} and Pt^{4+} in these three systems are nearly the same values (for example, in the case of Pt^{2+} , the range of their values is between 1.0×10^{-9} and $1.5 \times 10^{-9} \text{ m}^2 \text{ s}^{-1}$). Especially in the system of solutions without PVP, it has been remarkably observed that there are aggregates (or precipitates) in the colloidal solutions after the photoreduction of Pt ions. These results indicate that PVP is working as a stabilizer in the clustering of atoms to create their particles, and the regulation of the polymer concentration in the original solutions can make the size of the metal particles (or metal clusters) adequately controllable.

4.3. Diffusion Coefficients of the Chemical Species during the Photoreduction of PtCl_6^{2-} in Alcohol/Water Solution.

According to the Stokes–Einstein relationship, the diffusion coefficient D of a spherical molecule of radius r in a homogeneous nonviscous solvent with viscosity η is given by

$$D = kT/6\pi\eta r \quad (15)$$

From D of the Pt particles in the dilute and concentrated PVP solutions, r is calculated to be 3.69 and 4.62 nm from eq 15, respectively. These values correspond to the radius of aggregates of Pt particles, which we called “higher-order organization of superstructure of Pt particles” in our previous paper.³⁸ However, in the case of D for Pt^{2+} in the concentrated PVP solutions, we obtained $r = 0.139$ nm from eq 15. We found that this diameter ($2r = 0.278$ nm) of PtCl_4^{2-} is very close to the diameter from the crystallographic data (0.278 nm) of the Pt atom. Furthermore, as for the Pt ionic species (Pt^{2+} or Pt^{4+}) in the concentrated PVP solutions, D of Pt^{4+} is smaller than that of Pt^{2+} . This difference may be explained by the different numbers of Cl atoms coordinated to the Pt atom as well as the different electric charges, which cause a different solvation structure of water molecules around their ionic species. Thus, the size of the Pt ionic species with higher charges seems to be larger in the solvation structure.

Parts a and b of Figure 9 show the TEM images of Pt particles produced in the dilute and the concentrated PVP mixtures of 1/1 water and ethanol solutions by photoirradiation for 110 min, respectively. As is shown in the images, the size distribution of the diameter in the case of the concentrated PVP solution was sharp. The average diameter was 2.2 nm in the dilute PVP

(38) Hashimoto, T.; Saijo, K.; Harada, M.; Toshima, N. *J. Chem. Phys.* **1998**, *109*, 5627.

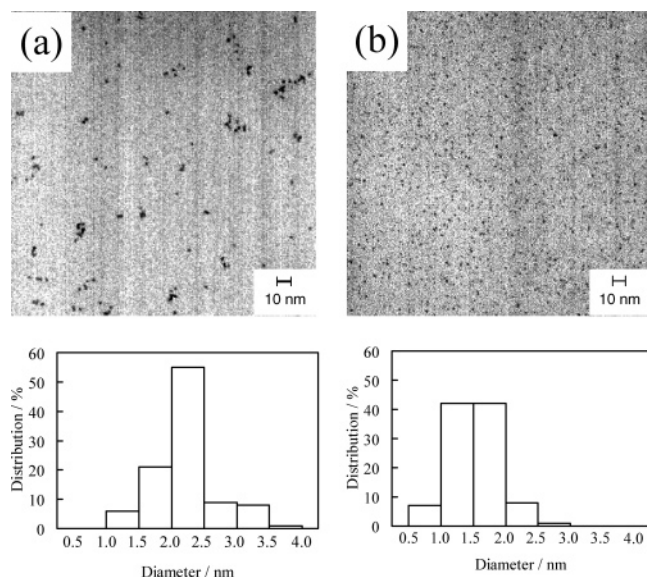


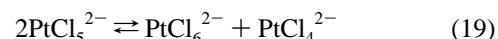
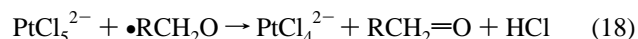
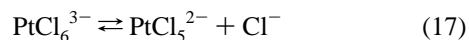
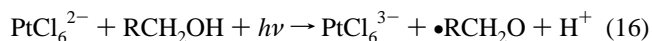
Figure 9. TEM images and distributions of the diameter extracted from the corresponding image for the Pt particles produced in (a) the dilute PVP solution and (b) the concentrated PVP solution by photoreduction. A 1/1 solution of water and ethanol was used as the solvent. The photoreduction was carried out for 110 min.

solutions and 1.5 nm in the concentrated PVP solutions, respectively. It is remarkable that there is a larger effect of the polymer concentration on the productivity and dispersity of the Pt particles under the photoreduction process.

The relative sizes of Pt particles prepared in different concentrations of PVP solution from the TEM measurement ($2r = 2.2$ nm for the dilute solution, and $2r = 1.5$ nm for the concentrated solution) are opposite those expected from D of the Pt particles ($2r = 7.38$ nm for the dilute solution, and $2r = 9.24$ nm for the concentrated solution). This discrepancy may be explained as follows. The radius from the TEM observation corresponds to the size of the metallic cores,^{39–41} but it does not include a polymer layer adsorbed on the surface of the particles. On the other hand, the hydrodynamic radius from the D value should include the thickness of the polymer layer. The smaller radius in the dilute solution may indicate that the thickness of the polymer layer adsorbed on the particle in the dilute PVP solution is smaller than in the concentrated PVP solution. In fact, the thickness of the adsorbed polymer layer has been determined by combining TEM measurements with other analytical methods. For example, the radius from TEM images and that from scanning tunneling microscopy (STM) techniques were used to estimate the thickness of the adsorbed polymer layer.⁴¹ It was determined from these techniques that the layer thickness of the tetraalkylammonium-stabilized Pd clusters was found to be 0.65–2.20 nm and its thickness depends on the length of the alkyl chain of tetraalkylammonium ions.⁴¹ Recently, a combination of TEM and dynamic light scattering (DLS) was carried out to study the structure of polymer–metal particles.^{42–44} The structure of gold–dendrimer nanocomposites prepared by laser irradiation was investigated by a combination of TEM and DLS, indicating that

they consist of gold nanoparticles covered by dendrimers as a monolayer with a thickness of 2.4–5.4 nm.⁴⁴ The measurement of D by the TG method is another convenient method to study the adsorbed polymer layer on the nanoparticles.

Here we additionally mention the effect of the inclusion of ethanol in these PVP systems. In previous studies,^{45–47} the initial step in the photoreduction from PtCl_6^{2-} to Pt^0 has been well investigated: Pt^{4+} is reduced to Pt^{3+} along with the simultaneous oxidation of alcohols (eq 16), which is subsequently transformed to Pt^{2+} by further reduction (eq 18) and disproportionation (eq 19) via formation of PtCl_5^{2-} complexes (eq 17).



This mechanism suggests that the oxidation potential and the viscosity of alcohols affect the rate of PtCl_4^{2-} formation, because their properties change the rate of the reduction from PtCl_6^{2-} to PtCl_6^{3-} (eq 16) and the encounter of two PtCl_5^{2-} complexes (eq 19). As a result, the inclusion of alcohols in the PVP systems enhances the reduction rate from PtCl_6^{2-} to PtCl_4^{2-} , and PtCl_6^{2-} is completely transformed to Pt^0 particles in aqueous alcoholic solutions. The size of the created Pt^0 particles is independent of the properties of the alcohols used in the photoreduction of PtCl_6^{2-} .¹⁵

For investigating the effect of ethanol, we have performed the following experiment. Photoirradiation with UV light of the solutions without ethanol was carried out for the first 30 min, and then ethanol was added to the obtained solution. As a result, the species grating signal appeared immediately after the ethanol was introduced into the system. This indicates that the ethanol is a more efficient reducing agent to enhance the rate of the reduction from PtCl_6^{2-} to PtCl_4^{2-} , which is observed in the step between parts a and b of Figure 3.

The reduction from PtCl_4^{2-} to Pt^0 atoms is a slower process, compared with the reduction from PtCl_6^{2-} to PtCl_4^{2-} . The reduction of PtCl_4^{2-} to Pt^0 atoms proceeds in two steps:³³ one is dissociation of Cl from PtCl_4^{2-} , and the other is reduction of Pt^{2+} to Pt^0 atoms. In the latter process, both Pt^{2+} and Pt^0 coexist in the solutions. Once a Pt^0 – Pt^0 bond is formed, the association of Pt^0 atoms into Pt^0 – Pt^0 oligomeric clusters is activated to create a Pt particle. This clustering process can be observed in the step between parts c and j of Figure 3.

4.4. Particle Formation Mechanism during Photoreduction of PtCl_6^{2-} . Figure 10 illustrates the Pt particle formation schemes in PVP solutions during the photoreduction by UV light of PtCl_6^{2-} to Pt particles. Figure 10a presents the ionic state of PtCl_6^{2-} in the solutions before the UV irradiation. Once the UV irradiation is performed, the rapid reduction of PtCl_6^{2-} to PtCl_4^{2-} via PtCl_5^{2-} occurs and PtCl_4^{2-} coexists in the solutions, as shown in Figure 10b. The transformation of PtCl_6^{2-} to PtCl_4^{2-} is complete within 1 min, which corresponds to the route from the spectrum of part a to that of part b of Figure 3, and only PtCl_4^{2-} exists in the solution, as shown in Figure 10c. It is obvious that PtCl_4^{2-} is

(39) Tadd, E.; Zeno, A.; Zubris, M.; Dan, N.; Tannenbaum, R. *Macromolecules* **2003**, *36*, 6497.

(40) Sidorov, S. N.; Bronstein, L. M.; Valetsky, P. M.; Hartmann, J.; Colfen, H.; Schnablegger, H.; Antonietti, M. *J. Colloid Interface Sci.* **1999**, *212*, 197.

(41) Retz, M. T.; Helbig, W.; Quaiser, S. A.; Stimming, U.; Breuer, N.; Vogel, R. *Science* **1995**, *267*, 367.

(42) Zheng, J.; Stevenson, M. S.; Hikida, R.; Van Patten, P. G. *J. Phys. Chem. B* **2002**, *106*, 1252.

(43) Holzinger, D.; Kickelbick, G. *Chem. Mater.* **2003**, *15*, 4944.

(44) Hayakawa, K.; Yoshimura, T.; Esumi, K. *Langmuir* **2003**, *19*, 5517.

(45) Grivin, V. P.; Khmelinski, I. V.; Plyusnin, V. F.; Blinov, I. I.; Balashev, K. P. *J. Photochem. Photobiol., A* **1990**, *51*, 167.

(46) Grivin, V. P.; Khmelinski, I. V.; Plyusnin, V. F. *J. Photochem. Photobiol., A* **1990**, *51*, 379.

(47) Grivin, V. P.; Khmelinski, I. V.; Plyusnin, V. F. *J. Photochem. Photobiol., A* **1991**, *59*, 153.

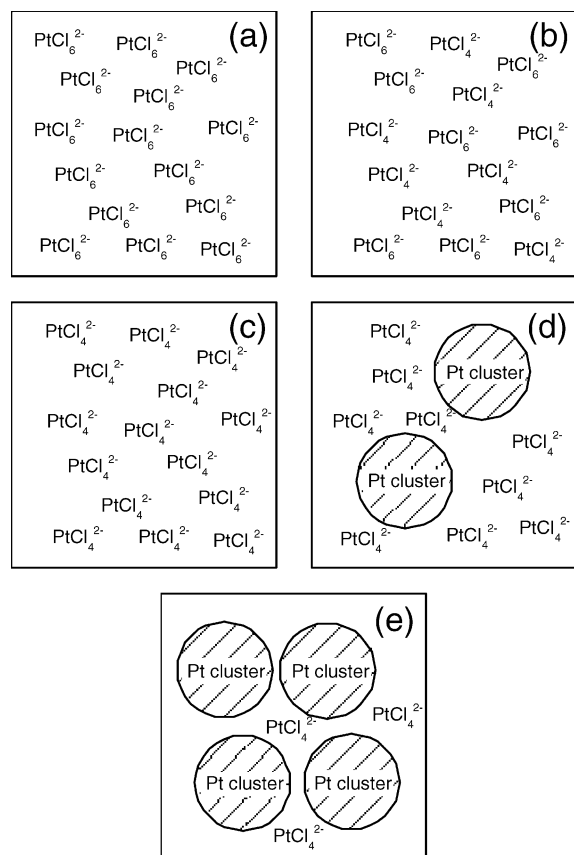


Figure 10. Schematic illustration of the photoreduction process of the Pt-containing solution (ethanol/water, 1/1 (v/v)) before and after UV irradiation. This illustration represents the state of the Pt ionic complexes as well as the Pt nanoparticles at the early stage of the photoreduction process.

much more stable in the aqueous solutions under long-time UV irradiation than PtCl_6^{2-} . Parts d and e of Figure 10 show the remaining PtCl_4^{2-} during the long-time UV irradiation and the

increasing number of created Pt particles associated with the Pt^0 atoms in the course of time, respectively. This feature reflects the decay of the species grating signal biexponentially and the increase of the signal intensity due to the Pt particle absorption, as shown in Figure 3c–j. This particle formation scheme in PVP solutions is consistent with our recent result.³³

5. Conclusion

The photoreduction of Pt^{4+} in PVP aqueous solution and formation of Pt particles were investigated by using the laser-induced TG method. The diffusion coefficients (D) of the Pt ionic species and the Pt particles during the photoreduction of PtCl_6^{2-} were measured. The TG signal of PtCl_6^{2-} solution before UV irradiation is composed of three kinds of contributions, the thermal grating, the species grating due to the creation of PtCl_4^{2-} , and the species grating due to the consumption of PtCl_6^{2-} . Upon UV irradiation, the TG signal due to the diffusion of Pt particles appears just after the TG signal due to Pt^{4+} being diminished and the transformation of Pt^{4+} to Pt^{2+} being completed within a few minutes. This result indicates that the gradual clustering of Pt atoms into Pt particles occurs, because the reduction from PtCl_4^{2-} to Pt^0 atoms is a slower process, compared with the reduction from PtCl_6^{2-} to PtCl_4^{2-} . With increasing time of UV irradiation, the TG signal intensity increases while the diffusion coefficient (D_{particle}) does not change. This suggests that the number of Pt particles increases, but the size of the Pt particles with polymer layers remains unchanged, in the course of time for UV irradiation. Finally, the translational diffusion of Pt particles with polymer layers is controlled by the amount of the protective polymer PVP.

Acknowledgment. We are grateful to Prof. S. Isoda at the Institute for Chemical Research, Kyoto University, for the TEM observations. A part of this work was supported by the “Nanotechnology Support Project” of the Ministry of Education, Culture, Sports, Science and Technology (MEXT), Japan.

LA061663I